



OPEN ACCESS

EDITED BY

Dongliang Xiao,
South China University of Technology,
China

REVIEWED BY

Qiang Fan,
Shanghai Jiao Tong University, China
Qiushi Cui,
Chongqing University, China

*CORRESPONDENCE

Yuanshi Zhang,
yuanshizhang@seu.edu.cn

SPECIALTY SECTION

This article was submitted to Smart
Grids,
a section of the journal
Frontiers in Energy Research

RECEIVED 07 August 2022

ACCEPTED 22 August 2022

PUBLISHED 13 September 2022

CITATION

Zhang Y, Wang L, Struthers C and Hu Q
(2022), A novel two-phase load
compensation method under
unbalanced voltages for renewable
energy integration.
Front. Energy Res. 10:1013585.
doi: 10.3389/fenrg.2022.1013585

COPYRIGHT

© 2022 Zhang, Wang, Struthers and Hu.
This is an open-access article
distributed under the terms of the
[Creative Commons Attribution License
\(CC BY\)](#). The use, distribution or
reproduction in other forums is
permitted, provided the original
author(s) and the copyright owner(s) are
credited and that the original
publication in this journal is cited, in
accordance with accepted academic
practice. No use, distribution or
reproduction is permitted which does
not comply with these terms.

A novel two-phase load compensation method under unbalanced voltages for renewable energy integration

Yuanshi Zhang^{1*}, Liwei Wang², Chris Struthers³ and Qinran Hu¹

¹School of Electrical Engineering, Southeast University, Nanjing, China, ²School of Engineering, University of British Columbia, Kelowna, BC, Canada, ³StruthersTech, Penticton, BC, Canada

This paper explores new design methods for correcting unbalanced power distribution networks in order to improve the power quality and reliability for sensitive industrial loads. While traditional compensators typically need to be connected to all the three phases of the AC network, this paper proposes a novel three-phase voltage balancing compensator that can operate with a connection to only two of the three phases. The new concept is based on the phasor symmetrical component theory, which can be implemented using either mechanically switched reactors (MSRs), TCRs (thyristor-controlled reactors) or VSCs (Voltage source converters). Three methods are presented to calculate the value of the proposed two-phase compensator, i.e., discrete solution, analytical solution and novel simplified solution. The discrete solution is solved via the exhaustive search method, which was successfully used by StruthersTech to correct the power quality of an unbalanced industrial power system. The analytical solution is based on the nodal voltage of analysis method. The simplified solution derives a practical albeit approximated relationship between the negative sequence source voltage and zero sequence load voltage, thus avoiding the need to solve nonlinear equations. Dynamic simulations are implemented using MATLAB/Simulink Simscape Blockset to validate the effectiveness of the proposed two-phase voltage balancing method.

KEYWORDS

mechanically switched reactors (MSRs), novel simplified method, thyristor controlled reactors (TCRs), voltage compensation, voltage source converters (VSCs), negative sequence compensation, zero sequence compensation

1 Introduction

With the large-scale intermittent renewable energy integrating into the smart grids, electrical engineers and researchers have heightened their level of concentration to power quality problem (Chen et al., 2020; Xiao et al., 2021; Hu et al., 2022a; Hu et al., 2022b). Power quality can be defined as the supply of adequately high-grade electrical utility services to the consumer/customer. To guarantee the power quality is one of the fundamental tasks at both transmission and distribution levels. Power quality

problems, especially voltage unbalance, have attracted wide attention, and a lot of research has been carried out on this topic (Fuchs and Masoum, 2008).

The adverse effects of the voltage unbalance are normally less serious than the current unbalance. Nevertheless, the loads and power electronics equipment may suffer more from the voltage unbalance (Xu et al., 2010). The negative impact of voltage unbalance on power grid and equipment such as induction motors and power electronic converters and drives has been studied in depth (Wang, 2001; Lee et al., 2006; Wei et al., 2022). Further, the available capacity of transformers and generators is negatively impacted by voltage unbalance, increasing the burden on the utility. Therefore, voltage compensation of non-linear and/or poor power factor loads and load balancing is an important issue in the modern power distribution system (Kazmierkowski, 2007). Normally, single-phase loads in a distribution system that are not consistently balanced between all three phases will result in unbalanced voltage at the load point of utilization (Woll, 1975). This is particularly true in terms of rural electric power grids with long distribution cables and/or fed by induction machines actuated by wind turbine generators. Moreover, large urban power grids also suffer from unbalanced voltage issues (Muljadi et al., 1999), (Muljadi, 1984).

Amongst the previous works related to the correction of the power quality, unbalanced voltage compensation has already been well studied. In (Peng and Lai, 1996; Akagi et al., 1999; Mishra et al., 2001), different compensation methods adopting instantaneous reactive power theory for shunt power filters are proposed. The loads in an unbalanced three-phase four-wire system are compensated with a static VAR compensator (SVC) (IEEE Special Stability Controls Working Group, 1994; Flores et al., 2009; Sun et al., 2011; Mi et al., 2018) combined with a series active filter in (Lee and Wu, 2000). In (Alkayyali and Ghaeb, 2019), a hybrid Particle Swarm Optimization–Artificial Neural Network algorithm is proposed to deal with the voltage unbalance issue by regulating the firing angles of thyristor controlled reactors (TCRs). The unbalanced voltage problem in distribution system is overcome by the dynamic voltage restorer (DVR), which is a power-electronic device that can protect sensitive loads from unprepared contingencies (Ghosh and Ledwich, 2002; Omar and Rahim, 2012; Sadigh and Smedley, 2012). Static VAR compensators (STATCOMS) are widely used for unbalanced voltage/current compensation in (Xu et al., 2010), (Escobar et al., 2001; Struthers, 2001; Mishra et al., 2007). In (Xu et al., 2010), an instantaneous power theory is used with three control schemes for voltage and current compensation. Two kinds of compensation strategies are proposed for unbalanced and distorted voltages in (Mishra et al., 2007). However, all of the existing literatures need to use three-phase compensators for voltage compensation. In this work, a novel two-phase voltage balancing compensator is proposed based on the phasor symmetrical component

theory, which can be realized by mechanically switched reactors (MSRs), TCRs, or Voltage source converters (VSCs). The two-phase compensator has the potential to significantly reduce the capital investment cost.

This work focuses on developing the algorithm of a novel two-phase compensator, which can be placed at any two phases. The key properties of the proposed algorithm and the overall contributions of the paper are summarized as follows:

- 1) The algorithm of the proposed novel two-phase compensator can be applied to various kinds of electrical devices, i.e., MSRs, TCRs as well as VSCs.
- 2) Three methods are presented to calculate the value of the proposed two-phase compensator, i.e., exhaustive search solution, exact analytical solution, and simplified analytical solution.
- 3) The discrete solution, which is very easy to implement, has been field-tested by StruthersTech at an operating Gold Mine.
- 4) The analytical solution applies the nodal voltage of analysis.
- 5) The novel simplified solution avoids calculating the nonlinear equations of the analytical solution and greatly reduces the calculation burden.

2 Discrete and analytical solutions using MSR

In order to illustrate the proposed voltage compensation method, a three-phase, three-wire test system including a 150/11kV Delta-Wye connected power transformer is considered, as shown in Figure 1. It is noted that the Delta-Wye transformer connection is widely used in the distribution system to eliminate the triplen harmonics from the primary side of the transformer. It is assumed that the three-phase load are unbalanced with equal load impedances and back Electro-Motive Forces (EMFs). The three-phase load is connected in ungrounded Wye or Delta connection. The goal is to balance the line-to-line voltage at the load terminal.

The corresponding three-phase equivalent diagram of Figure 1 is given in Figure 2, where V_{AS} , V_{BS} , V_{CS} are the unbalanced source voltages of phases A, B and C converted to the secondary side; R_T and X_T are the equivalent resistances and reactances of the transformer converted to the secondary side; V_{AL} , V_{BL} , V_{CL} are the load voltages of phases A, B and C, respectively; X_A , X_B , X_C are the (equivalent) MSRs to compensate the unbalanced voltages of phases A, B and C, respectively. Throughout, this paper, bold non-italic letter is used to represent a phasor.

It is assumed that the power network and the step-down transformer is represented by unbalanced three-phase voltage source with the neutral point connected to ground (directly or through impedance) as shown in Figure 2.

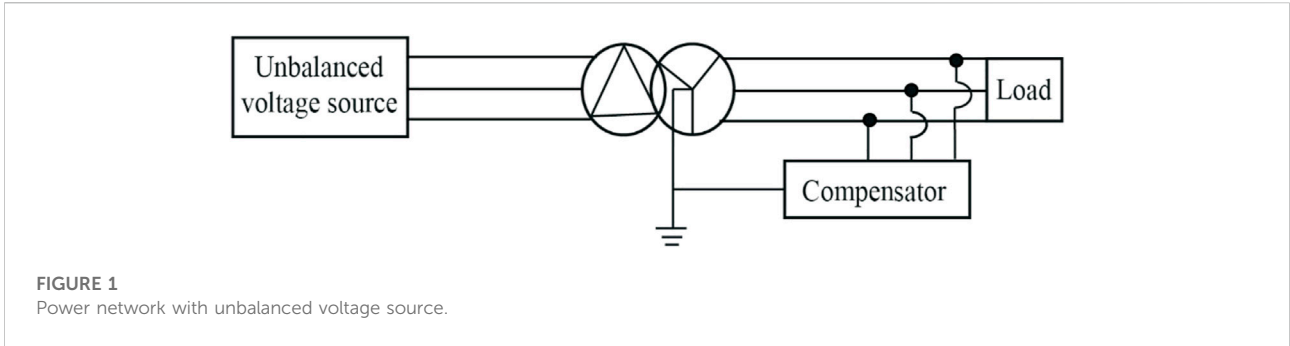


FIGURE 1 Power network with unbalanced voltage source.

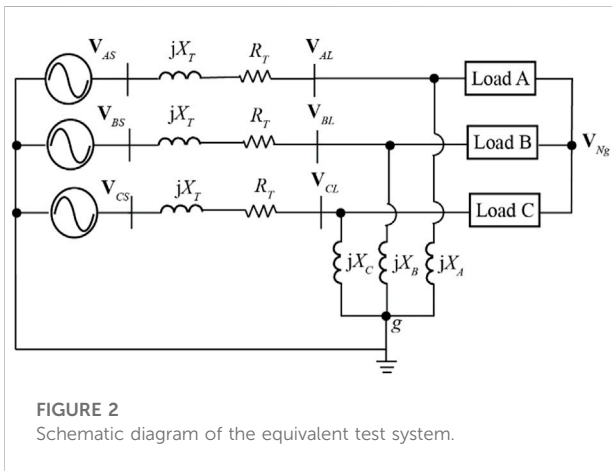


FIGURE 2 Schematic diagram of the equivalent test system.

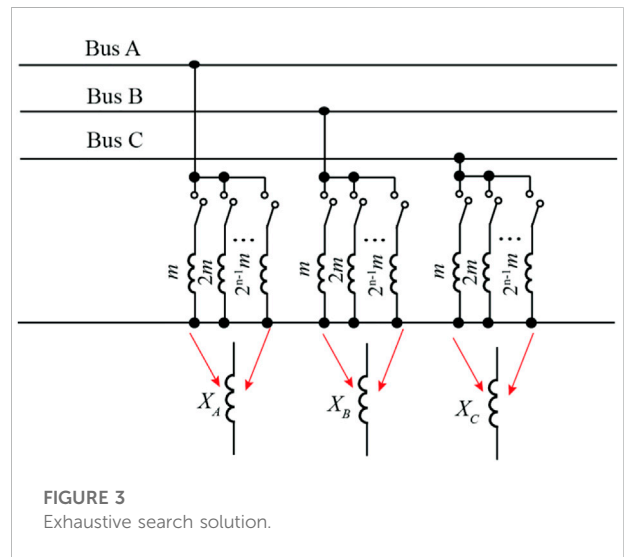


FIGURE 3 Exhaustive search solution.

2.1 Line-line voltage balancing

In the following, a novel voltage balancing method is proposed based on the phasor symmetrical component theory. According to the symmetrical component theory, the three phase load voltages can be decomposed as

$$\mathbf{V}_{AL} = \mathbf{V}_{AL,1} + \mathbf{V}_{AL,2} + \mathbf{V}_{AL,0} \tag{1}$$

$$\mathbf{V}_{BL} = \mathbf{V}_{BL,1} + \mathbf{V}_{BL,2} + \mathbf{V}_{BL,0} \tag{2}$$

$$\mathbf{V}_{CL} = \mathbf{V}_{CL,1} + \mathbf{V}_{CL,2} + \mathbf{V}_{CL,0} \tag{3}$$

where $\mathbf{V}_{iL,1}$ represents positive sequence load voltage of phase i ($i = A, B, C$); $\mathbf{V}_{iL,2}$ denotes negative sequence load voltage, and $\mathbf{V}_{iL,0}$ gives zero sequence load voltage. In Eqs 1–3, the zero sequence components, i.e. $\mathbf{V}_{AL,0}, \mathbf{V}_{BL,0}, \mathbf{V}_{CL,0}$, are all equal, based on symmetrical component theory. The load line-line voltage can be calculated as

$$\mathbf{V}_{AL} - \mathbf{V}_{BL} = \mathbf{V}_{AL,1} - \mathbf{V}_{BL,1} + \mathbf{V}_{AL,2} - \mathbf{V}_{BL,2} \tag{4}$$

$$\mathbf{V}_{BL} - \mathbf{V}_{CL} = \mathbf{V}_{BL,1} - \mathbf{V}_{CL,1} + \mathbf{V}_{BL,2} - \mathbf{V}_{CL,2} \tag{5}$$

$$\mathbf{V}_{CL} - \mathbf{V}_{AL} = \mathbf{V}_{CL,1} - \mathbf{V}_{AL,1} + \mathbf{V}_{CL,2} - \mathbf{V}_{AL,2} \tag{6}$$

If the difference of the negative sequence components, i.e., $\mathbf{V}_{AL,2} - \mathbf{V}_{BL,2}, \mathbf{V}_{BL,2} - \mathbf{V}_{CL,2}$, and $\mathbf{V}_{CL,2} - \mathbf{V}_{AL,2}$ in Eqs 4–6

are compensated to be zero, the line-line voltages are balanced. Thus, the equal negative sequence components, i.e., $\mathbf{V}_{AL,2} = \mathbf{V}_{BL,2} = \mathbf{V}_{CL,2}$, will lead to balanced three-phase load voltage. It is noted that the negative sequence components, $\mathbf{V}_{AL,2}, \mathbf{V}_{BL,2}, \mathbf{V}_{CL,2}$, have equal magnitudes with $2\pi/3$ phase shift due to symmetrical component theory. Therefore, the negative sequence components, $\mathbf{V}_{AL,2}, \mathbf{V}_{BL,2}, \mathbf{V}_{CL,2}$ should be all equal to zero (the magnitudes of $\mathbf{V}_{AL,2}, \mathbf{V}_{BL,2}, \mathbf{V}_{CL,2}$ are zero) in order to achieve three-phase balanced load voltage.

2.2 Exhaustive search solution

In the exhaustive search solution, each phase of the compensator consists of n number of parallel reactors controlled by the mechanical switches, as shown in Figure 3. The impedance values of the reactors in each phase are given as $m, 2 \times m, \dots, 2^{n-1} \times m$. Thus, there are numerous potential reactor combinations: 2^n values of the equivalent reactor impedances (X_A, X_B, X_C in Figures 2, 3) can be produced for each phase, and then there are 2^{3n} values of the three-phase

compensator. The exhaustive search method is used to select the best combination of reactors by controlling the combination of the turned-on switches to generate the smallest negative sequence voltage component in Eqs 4–6. The advantage of the exhaustive search solution is straightforward implementation for various scenarios of unbalanced voltages. The exhaustive solution is also extremely robust; if one or more reactors or switching devices are out of service or failing to respond, the algorithm can select the optimal combination with the remaining responsive reactors on the next calculation. However, the disadvantage of the exhaustive search method is its finite resolution and heavy computational burden, leading to high requirement of digital computing hardware.

2.3 Exact analytical solution

2.3.1 No-load scenario

In this subsection, the exact analytical solution of the compensator for no-load scenario is derived. When the system given in Figure 2 is operated without any load, it can be decoupled into three single phase equivalent circuits to facilitate the compensator impedance solution. The load voltage of each phase is given by

$$V_{AL} = \frac{jX_A}{R_T + j(X_T + X_A)} V_{AS} \tag{7}$$

$$V_{BL} = \frac{jX_B}{R_T + j(X_T + X_B)} V_{BS} \tag{8}$$

$$V_{CL} = \frac{jX_C}{R_T + j(X_T + X_C)} V_{CS} \tag{9}$$

Thereby, the negative sequence component of phase A can be calculated by

$$V_{AL,2} = \frac{1}{3} \left[\frac{jX_A V_{AS}}{R_T + j(X_T + X_A)} + a^2 \frac{jX_B V_{BS}}{R_T + j(X_T + X_B)} + a \frac{jX_C V_{CS}}{R_T + j(X_T + X_C)} \right] \tag{10}$$

where $V_{AL,2}$ is the negative sequence component of load voltage at phase A; $a = e^{j2\pi/3}$. The impedance values, X_A , X_B and X_C , can be solved by setting both the real and imaginary parts of $V_{AL,2}$ in Eq. 10 to be zero.

2.3.2 Loaded scenario

For the loaded scenario, as shown in Figure 2, the three-phase circuit cannot be decoupled. Without loss of generality, the three-phase asymmetrical load is represented by three-phase impedances of $R_{L,i} + jX_{L,i}$ ($i = A, B, C$) per phase. Applying nodal analysis to the compensated power network in Figure 2, one can obtain

$$\begin{bmatrix} Y_A & 0 & 0 & -Y_{N,A} \\ 0 & Y_B & 0 & -Y_{N,B} \\ 0 & 0 & Y_C & -Y_{N,C} \\ -Y_{N,A} & -Y_{N,B} & -Y_{N,C} & Y_N \end{bmatrix} \begin{bmatrix} V_{AL} \\ V_{BL} \\ V_{CL} \\ V_{Ng} \end{bmatrix} = \begin{bmatrix} \frac{V_{AS}}{R_T + jX_T} \\ \frac{V_{BS}}{R_T + jX_T} \\ \frac{V_{CS}}{R_T + jX_T} \\ 0 \end{bmatrix} \tag{11}$$

where $Y_{N,i} = \frac{1}{R_{L,i} + jX_{L,i}}$ stands for the load admittance of phase i ($i = A, B, C$); $Y_i = \frac{1}{R_T + jX_T} + \frac{1}{R_{L,i} + jX_{L,i}} + \frac{1}{jX_i}$ is the self admittance of phase i ; $Y_N = \frac{3}{R_L + jX_L}$ is the self admittance of the load neutral point; and V_{Ng} is the voltage of load neutral point. The three-phase load voltages (V_{AL} , V_{BL} and V_{CL}) can be solved from Eq. 11. The negative sequence component of phase A is obtained by

$$V_{AL,2} = \frac{1}{3} (V_{AL} + a^2 V_{BL} + a V_{CL}) \tag{12}$$

The compensator reactances, i.e., X_A , X_B and X_C , can be solved by combining Eqs 11, 12 and setting $V_{AL,2}$ in Eq. 12 to be zero. It is noted that this method applies to both balanced and unbalanced loads.

2.3.3 Degree of freedom

As $V_{AL,2}$ is a phasor, one needs to set both the real and imaginary parts to be zero. Thus, two equations will be obtained. Since two variables are needed for the two equalities yielding to a unique solution, only two-phase compensating reactors from X_A , X_B , X_C are required. In other words, the proposed compensation method requires only two-phase MSR to be installed in the unbalanced system.

Compared to the exhaustive search method, the results of the analytical solution can produce smaller negative sequence component and thus the voltage quality is better. However, the values of the compensating reactors need to be updated when the unbalanced voltage source and the load vary.

Normally recognizing $R_T + jX_T \ll R_L + jX_L$, Eq. 11 can be simplified into Eqs 7–9. Thus, the analytical solution of the loaded scenario is very similar to the unloaded scenario. Thus, the solution for the unloaded condition can be used to design the voltage balancing compensator for the loaded condition. It is noted that sometimes the loads are PQ type. Thus, one needs to calculate the load impedance using the equations below:

$$R_L = \frac{V^2 P}{P^2 + Q^2} \tag{13}$$

$$X_L = \frac{V^2 Q}{P^2 + Q^2} \tag{14}$$

3 Article types

The exact analytical solution, introduced in the previous section, require to solve 2×2 nonlinear equations from Eqs 10,

12. Numerical solution methods, for example, Newton-Raphson or Gauss-Seidel method can be used to solve them iteratively. However, this increase the computational burden of the digital control hardware of the compensator. In this section, a novel simplified analytical solution is proposed to avoid the solution of nonlinear equations for the compensator design. This simplified solution is based on the relationship between the negative sequence source voltage before compensation and zero-sequence load voltage after compensation. The simplified analytical solution is derived based on no-load scenario since the analytical solution of the loaded scenario is very similar to the unloaded scenario due to $R_T + jX_T \ll R_L + jX_L$.

3.1 Relationship between negative sequence source voltage and zero sequence load voltage

As discussed in Section 2.3.3, only two-phase compensation reactors are required. Without loss of generality, it is assumed that the compensators are installed on phases A and B. Assuming the zero-sequence component of V_{AS} before compensation is small and negligible (as would be the case with any three-wire industrial load utilizing a transformer with a delta winding), the three-phase load voltages from (7)–(9) can be written as

$$V_{AL} = (V_{AS,1} + V_{AS,2})m \tag{15}$$

$$V_{BL} = (V_{AS,1}e^{-j2\pi/3} + V_{AS,2}e^{j2\pi/3})n \tag{16}$$

$$V_{CL} = (V_{AS,1}e^{j2\pi/3} + V_{AS,2}e^{-j2\pi/3}) \tag{17}$$

with

$$m = \frac{jX_A}{R_T + j(X_T + X_A)} \tag{18}$$

and

$$n = \frac{jX_B}{R_T + j(X_T + X_B)} \tag{19}$$

In Eqs 15–17, $V_{AS,1}$ and $V_{AS,2}$ are positive sequence and negative sequence components of V_{AS} , respectively.

The zero-sequence voltage $V_{AL,0}$ after compensation is written as $V_{AL,0} = \frac{1}{3}(V_{AL} + V_{BL} + V_{CL})$

Substituting (15)–(17) into (20) yields

$$V_{AL,0} = \frac{1}{3} [(V_{AS,1} + V_{AS,2})m + (V_{AS,1}e^{-j2\pi/3} + V_{AS,2}e^{j2\pi/3})n + (V_{AS,1}e^{j2\pi/3} + V_{AS,2}e^{-j2\pi/3})] \tag{21}$$

As $V_{AS,2} \ll V_{AS,1}$, ignoring $V_{AS,2}$ in (21) and substituting $e^{-j2\pi/3} = -\frac{1}{2} - \frac{\sqrt{3}}{2}j$ and $e^{j2\pi/3} = -\frac{1}{2} + \frac{\sqrt{3}}{2}j$ into (21) yield

$$V_{AL,0} = \frac{1}{3}V_{AS,1} \left[\left(m - \frac{n}{2} - \frac{1}{2}\right) + \left(-\frac{\sqrt{3}}{2}n + \frac{\sqrt{3}}{2}\right)j \right] \tag{22}$$

The negative sequence load voltage, $V_{AL,2}$, after compensation, should be equal zero. Based on (15)–(17) and (12), one can get

$$(V_{AS,1} + V_{AS,2})m + \left[V_{AS,1} \left(-\frac{1}{2} + \frac{\sqrt{3}}{2}j\right) + V_{AS,2} \right]n + \left[V_{AS,1} \left(-\frac{1}{2} - \frac{\sqrt{3}}{2}j\right) + V_{AS,2} \right] \tag{23}$$

From (23), the relationship between $V_{AS,1}$ and $V_{AS,2}$ is given by

$$V_{AS,2} = \frac{V_{AS,1} \left[-\left(m - \frac{n}{2} - \frac{1}{2}\right) + \left(-\frac{\sqrt{3}}{2}n + \frac{\sqrt{3}}{2}\right)j \right]}{m + n + 1} \tag{24}$$

As $|R_T + jX_T| \ll |X_A|$ and $|R_T + jX_T| \ll |X_B|$, one can obtain that $m \approx n \approx 1$. Thus, the denominator of (24) approximately equals 3. Thus, (24) is rewritten as

$$V_{AS,2} \approx \frac{1}{3}V_{AS,1} \left[-\left(m - \frac{n}{2} - \frac{1}{2}\right) + \left(-\frac{\sqrt{3}}{2}n + \frac{\sqrt{3}}{2}\right)j \right] \tag{25}$$

Comparing (25) with (12), it can be observed that the real part of $V_{AL,0}$ is the opposite of the real part of $V_{AS,2}$, while the imaginary parts of $V_{AL,0}$ and $V_{AS,2}$ are the same. Therefore, $V_{AL,0}$ can be expressed using the complex conjugate of $V_{AS,2}$ as

$$V_{AL,0} \approx -V_{AS,2}^* \tag{26}$$

where the superscript ‘*’ is complex conjugate operator.

3.2 Compensator design using simplified analytical solution

In this subsection, a simplified analytical solution based on the relationship between $V_{AS,2}$ and $V_{AL,0}$ in (26) is proposed. The compensator reactance values are calculated using the following procedure:

- 1) Without loss of generality, it is assumed that the compensation reactors are installed at both phases A and B.
- 2) Calculating the zero sequence load voltage $V_{AL,0}$ from the negative sequence source voltage $V_{AS,2}$ according to (26).
- 3) Since phase C is not compensated and negative sequence load voltages $V_{AL,2} = V_{BL,2} = V_{CL,2} = 0$ after compensation, the positive sequence load voltage $V_{CL,1}$ of phase C is calculated as
- 4) Deriving the positive sequence load voltages of phases A and B, based on the positive sequence load voltage $V_{CL,1}$ of phase C as

$$V_{CL,1} = V_{CL} - V_{AL,0} \tag{27}$$

$$V_{BL,1} = V_{CL,1} e^{j2\pi/3} \tag{28}$$

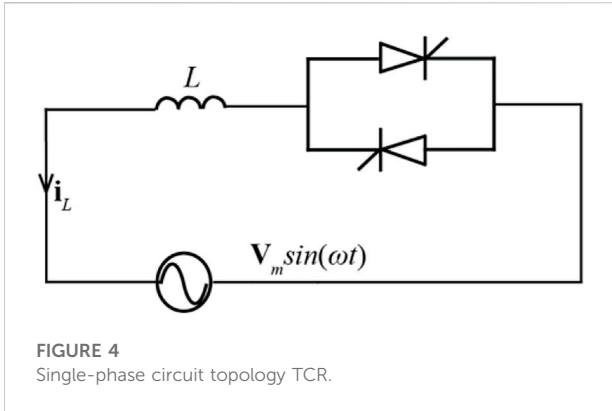


FIGURE 4 Single-phase circuit topology TCR.

TABLE 1 Parameters of the equivalent circuit of the martabe gold mine.

Symbol	Value
$V_{AS,1}$	$6.673 \times \sin(\omega t)$ kV
$V_{AS,2}$	$0.081 \times \sin(\omega t + 0.9628 \times \pi)$ kV
L	0.01 H
R_f	5 m Ω
L_f	690 μ H
X_T	0.0019H
R_T	0.1 m Ω

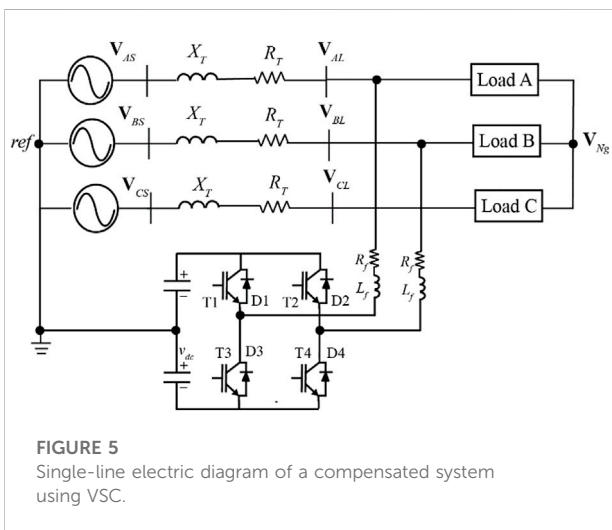


FIGURE 5 Single-line electric diagram of a compensated system using VSC.

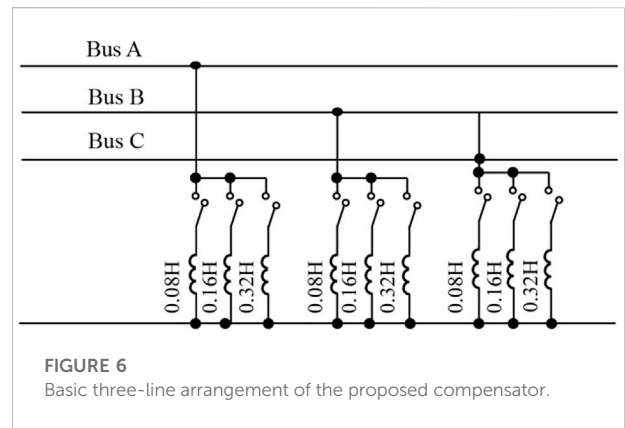


FIGURE 6 Basic three-line arrangement of the proposed compensator.

$$V_{AL,1} = V_{BL,1} e^{j2\pi/3} \tag{29}$$

5) Synthesizing the load voltages of phases A and B from their symmetrical components as

$$V_{AL} = V_{AL,0} + V_{AL,1} \tag{30}$$

$$V_{BL} = V_{AL,0} + V_{BL,1} \tag{31}$$

6) Determining the compensator impedance values of phases A and B under no-load scenario as

$$Z_A = \frac{V_{AL}}{V_{AS} - V_{AL}} (R_T + jX_T) \tag{32}$$

$$Z_B = \frac{V_{BL}}{V_{BS} - V_{BL}} (R_T + jX_T) \tag{33}$$

7) The compensator reactances of phases A and B are solved by taking the imaginary parts of Eqs 32, 33 as

$$X_A = \text{Im}(Z_A) \tag{34}$$

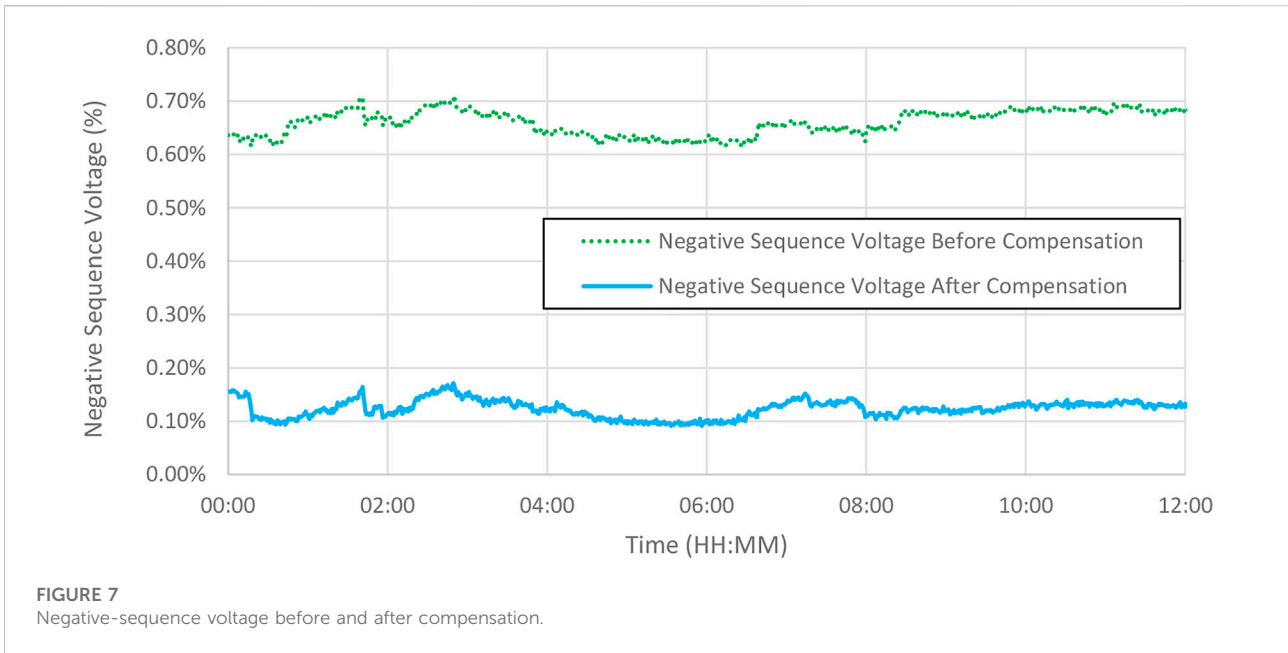
$$X_B = \text{Im}(Z_B) \tag{35}$$

It is noted that compared with the analytical solution of (10) or (12), the simplified analytical solution does not need to solve any nonlinear equations. Thus, the calculation burden of the digital control platform of the compensator is greatly reduced.

4 Compensator implementation using line commutated converter

In this section, the line commutated converter (LCC) is implemented to compensate the unbalanced voltages instead of the MSR, as introduced in Section 2 and Section 3. As a well-proven technology, thyristor controlled reactor (TCR) is used for the compensator implementation. Comparing with MSR proposed in Section 2, TCR has the advantage that the equivalent reactance value is continuous and can be updated conveniently with the changing system conditions.

The single-phase circuit topology of TCR is illustrated in Figure 4 (IEEE Special Stability Controls Working Group, 1994)–



(Flores et al., 2009), which mainly comprises of a pair of thyristors and a reactor.

It is noted that the detailed derivation.

With the detailed derivation in the Appendix, the equivalent fundamental frequency reactance $X_L(\beta)$ is given as

$$X_L(\beta) = \frac{V_m}{I_{L,1}} = \frac{\pi\omega L}{2\beta - \sin 2\beta} \quad (36)$$

where β is called the conduction angle, ω is the radian frequency, L is the inductance.

5 Compensator implementation using voltage source converter

The two-phase VSC to compensate the unbalanced voltage is shown in Figure 5. The advantage of the VSC is that it has smaller low order harmonics when compensating the grid voltage. Without loss of generality, it is assumed that a full-bridge converter is used as a two-phase VSC. The full-bridge converter can be installed at two arbitrary phases of the grid. In Figure 5, it is assumed that the VSC is installed at phases A and B. Both open-loop and closed-loop controls are designed to regulate the output voltage of the VSC so that the grid voltage at the load terminals are balanced.

For the open-loop control, the substitution principle is employed. To be more specific, the compensated load voltages (V_{AL} and V_{BL}) using the VSC should be equal to the compensated load voltages using MSR in Section 2 or Section

3. The following steps are performed to obtain the VSC AC voltage references Under the no-load condition.

- 1) The equivalent reactance values elaborated in Section 2 or Section 3 are calculated.
- 2) Employing the substitution principle, the compensated load voltages V_{AL} and V_{BL} are calculated from the MSR values X_A and X_B .

$$V_{AL} = V_{AS} \frac{X_A}{(X_T + X_A) - jR_T} \quad (37)$$

$$V_{BL} = V_{BS} \frac{X_B}{(X_T + X_B) - jR_T} \quad (38)$$

- 3) Finally, the AC voltage references, V_{AO} and V_{BO} , for phases A and B, respectively, can be obtained as

$$V_{AO} = V_{AS} - \frac{V_{AS} - V_{AL}}{R_T + jX_T} (R_f + j\omega L_f + R_T + jX_T) \quad (39)$$

$$V_{BO} = V_{BS} - \frac{V_{BS} - V_{BL}}{R_T + jX_T} (R_f + j\omega L_f + R_T + jX_T) \quad (40)$$

where R_f and L_f are the resistance and inductance of the filter shown in Figure 5.

In order to increase the accuracy and flexibility of the proposed method, closed-loop control is also designed. The negative-sequence voltage of phase A is the input of the PI controller and the output of the PI controller is added to the amplitude of VSC AC output voltage reference. The closed-loop control can flexibly deal with some unprepared disturbances such as load and source voltage variations.

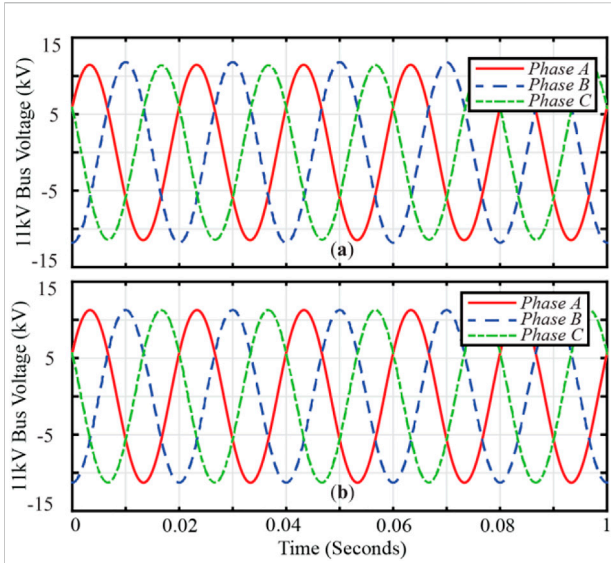


FIGURE 8
Three-phase voltage waveforms on 11 kV bus before and after compensation. (A) Three-phase voltage waveforms before compensation. (B) Three-phase voltage waveforms after compensation.

6 Simulation studies

The simulation system, as shown in Figure 1, chosen for the case studies is based on the power quality correction project for Martabe Gold Mine carried out by the Struthers Technical Solutions Ltd. (StruthersTech). Metering was performed on the 150 kV busbars at the Martabe substation, between Sibolga and Padang Sidempuan. The parameters of the equivalent circuit in Figure 2, the value of the inductor, i.e., L , of TCR in Figure 4 and the R_f and L_f in Figure 5 are given in Table 1.

6.1 Case A: Exhaustive search solution using MSR

In the project of Power Quality Correction for Martabe Gold Mine, the Struthers Tech designed the exhaustive search solution using combinations of discrete inductor components to compensate the unbalanced voltages. The proposed compensators will be connected directly to the secondary terminals of the 150/11 kV power transformers. Each is connected in a 4-wire configuration, with a fully insulated neutral bus connected via cable. The load is mostly induction motor type, all fed from 11 kV step-down transformers having a primary Delta connection.

As shown in Figure 6, each phase of the proposed compensator is composed of three MSRs in parallel with the three inductors of 0.08 H, 0.16 H, and 0.32 H. Thereby,

TABLE 2 Ten unbalanced loads (Ω).

Moment	Phase A (j)	Phase B (jj)	Phase C (j)
1	7.620 + 2.142	7.20 + 2.142	7.629 + 2.332
2	7.619 + 2.147	7.639 + 2.347	7.622 + 2.147
3	7.527 + 2.140	7.527 + 2.148	7.527 + 2.120
4	7.494 + 2.144	7.494 + 2.144	7.466 + 2.174
5	7.580 + 2.157	7.580 + 2.247	7.594 + 2.157
6	7.600 + 2.145	7.550 + 2.145	7.600 + 2.145
7	7.530 + 2.131	7.530 + 2.131	7.760 + 2.125
8	7.492 + 2.175	7.492 + 2.175	7.492 + 2.55
9	7.487 + 2.148	7.499 + 2.148	7.487 + 2.448
10	7.475 + 2.142	7.472 + 2.142	7.479 + 2.262

there are 512 values of the equivalent compensators according to Section 2.2. Exhaustive search method is applied to find the desirable combination of MSRs, which yields the minimum negative sequence component of the load voltage. According to the calculated results, the optimal combination of MSRs is infinite for A phase (Compensator of phase A is not connected), 0.0457 H for B phase (all of the MSRs are connected), and 0.064 H for C phase (MSRs with the values of 0.08 H and 0.32 H are connected).

The negative sequence voltage before and after compensation over a 12-h time period is shown in Figure 7, which is a practical field result recorded by the StruthersTech. It can be seen from Figure 7 that, the negative sequence voltage on the uncompensated 11 kV bus without compensation can be up to nearly 0.7%. With the compensator designed by the StruthersTech in service, the negative sequence imbalance on the compensated 11 kV bus is reduced to less than 0.2%.

6.2 Case B: Exact analytical solution using MSR and TCR

For the analytical solution, the lower bound of the compensator of each phase is defined to be 0.0437H and the upper bound is infinite. The Matlab function “fmincon” can be used to solve this optimization problem by setting X_a , X_b and X_c to be three independent variables and the absolute value of $V_{AL,2}$ to be minimization function of fmincon

6.2.1 No-load condition using MSR

According to Eq. 10 in Section 2.3.1, the analytical compensator value calculated by the fmincon function is infinite for A phase, 0.0486 H for B phase, and 0.0560 H for C phase. The negative sequence voltage is minimized

TABLE 3 Analytical compensator values and negative sequence voltage after compensation.

Moment	Phase B (H)	Phase C (H)	Negative Voltage (%)
1	0.0493	0.0567	0.03
2	0.0492	0.0566	0.03
3	0.0493	0.0567	0.03
4	0.0493	0.0567	0.03
5	0.0493	0.0568	0.03
6	0.0494	0.0567	0.03
7	0.0493	0.0567	0.03
8	0.0493	0.0567	0.03
9	0.0492	0.0566	0.03
10	0.0493	0.0567	0.03

TABLE 4 Amplitudes and phase angles for the AC output voltage references of phases B and C.

	Phase B	Phase C
Amplitude	0.8206	0.6082
Phase angle (rad)	1.0568	-1.0582

from 80.64 V (1.24%) before compensation to 0.216 V (0.003%) after compensation by the analytical solution. The voltage waveforms on 11 kV bus before and after compensation is shown in Figure 8A,B respectively. From Figure 8B it can be observed that, the three-phase voltage waveforms after compensation is much more balanced than those before compensation as shown in Figure 8A.

6.2.2 Loaded condition using MSR

For the loaded condition, ten successive moments of the 11 kV bus with the unbalanced full-loaded loads are compensated using the analytical solution elaborated in Section 2.3.2. The resistive unbalanced loads over ten successive moments are given in Table 2. The analytical values of the compensator installed on phases B and C and negative sequence voltage after compensation are given in Table 3. From Table 3 it can be seen that the values of compensator under loaded condition are close to the compensator value of the unloaded condition.

6.2.3 Analytical solution using TCR

Similar to the MSRs in Case 6.2.1, TCRs are installed on B phase and C phase. Applying the method elaborated in Section 4, the conduction angles β to obtain the equivalent reactance for phase B and phase C are 0.44 rad and 1.34 rad respectively. The simulation result shows that the negative-sequence voltage is reduced to relatively small, which is 1.106 V (0.0168%).

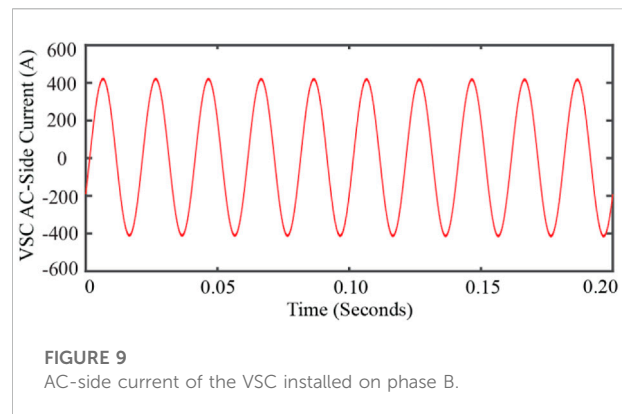


FIGURE 9 AC-side current of the VSC installed on phase B.

6.2.4 Case C: Simplified solution using VSC

Applying the simplified solution in Section 3, the inductances of the compensators in phase B and phase C are 0.0479 H and 0.0550 H, respectively. While the analytical calculation results of the inductance values are 0.0486 H for phase B and 0.0560 H for phase C. It can be seen that the simplified calculation result of the compensator is quite close to the analytical result. But the simplified solution does not need to solve the nonlinear equations so that it is easier to be implemented and has less computational burden.

After following the corresponding steps in Section 5, the amplitudes and phase angles for the AC voltage modulating indexes of phase B and phase C are given in Table 4.

From the simulation result, the negative-sequence voltage after compensated by the two-phase VSC is reduced to 1.444 V (0.021%). In addition, the AC-side current of the VSC installed on phase B is shown on Figure 8. From Figure 9 it can be seen that, the amplitude of the AC-side current is around 420 A.

7 Conclusion

In this work, a novel algorithm for two-phase voltage balancing compensator is proposed based on the phasor symmetrical component theory, which can be applied to MSRs, TCRs or VSCs. The proposed two-phase compensator can greatly reduce the investment cost compared to the traditional three-phase compensator. Three methods are proposed to calculate the value of the proposed two-phase compensator, i.e. discrete solution, analytical solution and novel simplified solution. The discrete solution has been proven in a field application by StruthersTech in the project of PLN Power Quality Correction for Martabe Gold Mine and is very easy to be implemented. The novel simplified solution can avoid calculating the nonlinear equations of the analytical solution, which can greatly reduce the calculated burden. The field work results as well as the dynamic simulations implemented with MATLAB/Simulink Simscape Blockset validate the accuracy and the effectiveness of the proposed two-phase voltage balancing method. It is noted that the proposed method can be used in both transmission system and distribution system with various topologies. The limitation of the proposed two-phase balancing method is that it cannot compensate the distorted voltage. Thus, the load compensation techniques under distorted voltages will be our future work.

Data availability statement

The original contributions presented in the study are included in the article/Supplementary Materials, further inquiries can be directed to the corresponding author.

Author contributions

YZ, CS, and LW contributed to the conception and design of the algorithm and case study. YZ and LW wrote the first draft of

the manuscript. QH contributed to manuscript revision and proofread and approved the submitted version.

Funding

This research is supported by the National Natural Science Foundation of China (51907026), Natural Science Foundation of Jiangsu Province, China (BK20190361), Key Research and Development Program of Jiangsu Province, China (BE2020081-2).

Acknowledgments

The authors would like to thank the National Natural Science Foundation of China (51907026), Natural Science Foundation of Jiangsu Province, China (BK20190361), Key Research and Development Program of Jiangsu Province, China (BE2020081-2).

Conflict of interest

The authors declare that the research was conducted in the absence of any commercial or financial relationships that could be construed as a potential conflict of interest.

Publisher's note

All claims expressed in this article are solely those of the authors and do not necessarily represent those of their affiliated organizations, or those of the publisher, the editors and the reviewers. Any product that may be evaluated in this article, or claim that may be made by its manufacturer, is not guaranteed or endorsed by the publisher.

References

- Akagi, H., Ogasawara, S., and Kim, H. (1999). The theory of instantaneous power in three-phase four systems: a comprehensive approach. *Proceeding. 34th Ind. Appl. Conference, Ind. Appl. Soc Annual Meeting, Phoenix, AZ, USA, Oct. 3-7* 1, 431-439.
- Alkayyali, M., and Ghaeb, J. (2019). Hybrid PSO-ANN algorithm to control TCR for voltage balancing. " IET Generation. *Transm. Distribution* 14 (5), 863-872.
- Chen, T., Pipattanasomporn, M., Rahman, I., Jing, Z., and Rahman, S. (2020). MATPLAN: A probability-based planning tool for cost-effective grid integration of renewable energy. *Renew. Energy* 156, 1089-1099. doi:10.1016/j.renene.2020.04.145
- Escobar, G., Mattavelli, P., and Stankovic, A. M. (2001). Reactive power and unbalance compensation using STATCOM with dissipativity-based control. *IEEE Trans. Control Syst. Technol.* 9, 718-727.
- Flores, P., Dixon, J., Ortuzar, M., Carmi, R., Barriuso, P., and Moran, L. (2009). Static Var compensator and active power filter with power injection capability, using 27-level inverters and photovoltaic cells. *IEEE Trans. Ind. Electron.* 56 (1), 130-138. doi:10.1109/tie.2008.2009513
- Fuchs, E. F., and Masoum, M. A. S. (2008). *Power quality in power systems and electrical machines*. San Diego, CA: Academic.
- Ghosh, A., and Ledwich, G. (2002). Compensation of distribution system voltage using DVR. *IEEE Trans. Power Deliv.* 17 (4), 1030-1036. doi:10.1109/tpwr.2002.803839
- Hu, Q., Han, R., Quan, X., Wu, Z., Tang, C., Li, W., et al. (2022a). Grid-forming inverter enabled virtual power plants with inertia support capability. *IEEE Trans. Smart Grid*, 1. doi:10.1109/TSG.2022.3141414
- Hu, Q., Liang, Y., Ding, H., Quan, X., Wang, Q., and Bai, L. (2022b). Topological partition based multi-energy flow calculation method for complex integrated energy systems. *Energy* 244, 123152. doi:10.1016/j.energy.2022.123152
- IEEE Special Stability Controls Working Group (1994). Static VAR compensator models for power flow and dynamic performance simulation. *IEEE Trans. Power Syst.* 9, 229-240.
- Kazmierkowski, M. P. (2007). *Power quality: Mitigation technologies in a distributed environment*. Berlin: Springer Science & Business Media.

- Lee, K., Jahns, T. M., Berkopec, W. E., and Lipo, T. (2006). Closed-form analysis of adjustable-speed drive performance under input-voltage unbalance and sag conditions. *IEEE Trans. Ind. Appl.* 42 (3), 733–741. doi:10.1109/tia.2006.872953
- Lee, S. Y., and Wu, C. J. (2000). Reactive power compensation and load balancing for unbalanced three-phase four-wire system by a combined system of an SVC and a series active filter. *IEE Proc. Electr. Power Appl.* 147 (6), 563–578. doi:10.1049/ip-epa:20000722
- Mi, Y., Ma, C., Fu, Y., Wang, C., Wang, P., and Loh, P. C. (2018). “The SVC additional adaptive voltage controller of isolated wind-diesel power system based on double sliding-mode optimal strategy. *IEEE Trans. Sustain. Energy* 9 (1), 24–34. doi:10.1109/tste.2017.2713700
- Mishra, M. K., Ghosh, A., Joshi, A., and Suryawanshi, H. M. (2007). A novel method of load compensation under unbalanced and distorted voltages. *IEEE Trans. Power Deliv.* 22 (1), 288–295. doi:10.1109/tpwrd.2006.881579
- Mishra, M. K., Joshi, A., and Ghosh, A. (2001). A new compensation algorithm for balanced and unbalanced distribution systems using generalized instantaneous reactive power theory. *Electr. Power Syst. Res.* 60, 29–37. doi:10.1016/s0378-7796(01)00166-3
- Muljadi, E. (1984). *Induction machine phase balancing by unsymmetrical voltage control*. Madison: University of Wisconsin.
- Muljadi, E., Batan, T., Yildirim, D., and Butterfield, C. P. (1999). “Understanding the unbalanced voltage problem in wind turbine generation,” in Conf. Rec. IEEE IAS Annu. Meeting, Phoenix, AZ, USA, 03–07 October 1999, 1359–1365.
- Omar, R., and Rahim, N. A. (2012). Voltage unbalanced compensation using dynamic voltage restorer based on super capacitor. *Int. J. Electr. Power & Energy Syst.* 43, 573–581. doi:10.1016/j.ijepes.2012.05.015
- Peng, F. Z., and Lai, J. S. (1996). Generalized instantaneous reactive power theory for three-phase power systems. *IEEE Trans. Instrum. Meas.* 45 (1), 293–297. doi:10.1109/19.481350
- Sadigh, A. K., and Smedley, K. M. (2012). “Review of voltage compensation methods in dynamic voltage restorer (DVR),” in Proceedings of the IEEE Power Energy Society General Meeting, San Diego, CA, USA, 22–26 July 2012, 1–8.
- Struthers, C. Three phase load balancing and power factor correction using a pulse width modulated static compensator. MS thesis. 2001.
- Sun, L. Y., Tong, S., and Liu, Y. (2011). Adaptive backstepping sliding mode H_{∞} control of static var compensator. *IEEE Trans. Control Syst. Technol.* 19 (5), 1178–1185. doi:10.1109/tcst.2010.2066975
- Wang, Y. J. (2001). Analysis of effects of three-phase voltage unbalance on induction motors with emphasis on the angle of the complex voltage unbalance factor. *IEEE Trans. energy Convers.* 16 (3), 270–275. doi:10.1109/60.937207
- Wei, C., Zhao, Y., Zheng, Y., Xie, L., and Smedley, K. (2022). Analysis and design of a non-isolated high step-down converter with coupled inductor and ZVS operation. *IEEE Trans. Ind. Electron.* 69 (9), 9007–9018. doi:10.1109/tie.2021.3114721
- Woll, R. F. (1975). Effect of unbalanced voltage on the operation of polyphase induction motors. *IEEE Trans. Ind. Appl.* 11, 38–42. doi:10.1109/tia.1975.349255
- Xiao, D., Chen, H., Wei, C., and Bai, X. (2021). Statistical measure for risk-seeking stochastic wind power offering strategies in electricity markets. *J. Mod. Power Syst. Clean Energy*.2021. doi:10.35833/MPCE.2021.000218
- Xu, Y., M Tolbert, L., Kueck, J. D., and Rizy, D. T. (2010). Voltage and current unbalance compensation using a static var compensator. *IET Pwr. Electr.* 3 (6), 977–988. doi:10.1049/iet-pel.2008.0094

Appendix A:

The triggering points of the thyristors are given by

$$\omega t = \alpha + k\pi \quad (\text{A1})$$

where α is the firing angle; ω is the radian frequency; and k is a non-negative integer.

The current flowing through the inductor is calculated by

$$L \frac{di_L}{dt} = V_m \sin(\omega t) \quad (\text{A2})$$

The general solution of Eq. 33 is written by

$$i_L = K - \frac{V_m}{\omega L} \cos(\omega t) \quad (\text{A3})$$

where K is the integration constant.

It is noted that i_L is zero at all the triggering point. Then we can get,

$$i_L = \frac{V_m}{\omega L} [\cos(\alpha + k\pi) - \cos(\omega t)] \quad (\text{A4})$$

It is noted that the current becomes zero again at $\omega t = (k+2)\pi - \alpha$. Thus, the conduction period is

$\omega t \in [\alpha + k\pi, (k+2)\pi - \alpha]$. The width of the current waveform is

$$(k+2)\pi - \alpha - (\alpha + k\pi) = 2(\pi - \alpha) = 2\beta \quad (\text{A5})$$

where β is called the conduction angle (IEEE Special Stability Controls Working Group, 1994).

Applying Fourier analysis to the reactor current, the amplitude of the fundamental frequency component is formulated as

$$\begin{aligned} I_{L,1} &= \frac{2}{\pi} \int_{\alpha}^{2\pi-\alpha} \frac{V_m}{\omega L} (\cos \alpha - \cos \theta) \cos \theta d\theta \\ &= \frac{V_m}{\pi \omega L} [2(\alpha - \pi) - \sin 2\alpha] \end{aligned} \quad (\text{A6})$$

Then the instantaneous value of fundamental wave is

$$i_{L,1} = I_{L,1} \cos(\omega t) = \frac{V_m}{\pi \omega L} (2\beta - \sin 2\beta) \sin\left(\omega t - \frac{\pi}{2}\right) \quad (\text{A7})$$

The conduction angle β for each TCR can be determined by Eq. A4 with Eqs 34, 35 of the two-phase compensators, respectively.